Magnetically coupled percutaneous connector for chronic electrical peripheral nerve stimulation and recording in awake rats

Jerico V. Matarazzo, Daniel T. Williams-Wynn, James B. Fallon, Sophie C. Payne

***Abstract*— A fast-growing field of neuroscience and medicine is the treatment of disease via electrical stimulation of the peripheral nervous system. Peripheral nerve stimulation delivers stimulation to nerves of the periphery where the target nerve can and is often located deep within the abdomen. Long-term preclinical animal models that demonstrate the safety and/or efficacy of electrical stimulation have predominantly used a skull mount to connect to neural interfaces. When targeting nerves of the extremities and abdomen, this mount location is less favourable due to its distance to the implant causing complications in surgery and to the longevity of the device *in vivo*. *Objective:* Here we aimed to develop and validate a chronic magnetic percutaneous connector designed for placement on the dorsal-lumbar aspect of the spine of awake, freely moving rats. *Methods:* A pedestal and external connector was developed, bench tested to assess for continuity, durability and disconnection forces, and validated in awake rats chronically implanted with an abdominal vagus nerve electrode array. The implanted pedestal and external connector were designed with custom PCBs, spring-loaded pins, magnets and biocompatible 3D printed housing. *Results:* The magnetic coupling mechanism allowed disconnection with minimal force, was highly reliable in maintaining electrical connection in awake rats and allowed recording of electrically evoked compound action potentials after chronic implantation. *Conclusion:* In conclusion, this percutaneous connector is a useful research tool for peripheral nerve stimulation studies. *Significance:* The connector described will allow investigation into the safety and efficacy of emerging neuromodulation therapies for the treatment of disease.**

Index Terms – 3D printing, implant, manufacturing, neuromodulation

Research reported in this publication was supported by the Bionics Institute Incubation Fund and from the National Health and Medical Research Council (APP2028605). The Bionics Institute acknowledge the support they receive from the Victorian Government through its Operational Infrastructural Support Program.

J.V.Matarazzo and D.T.Williams-Wynn are with Bionics Institute, VIC 3002, Australia (phone: (03) 9667 7500; e-mail: jmatarazzo@bionicsinstitute.org, dwilliams-wynn@bionicsinstitute.org)

S.C.Payne is with Bionics Institute, VIC 3002, Australia and Medical Bionics Department, University of Melbourne, VIC 3010, Australia (phone: (03) 9667 7500; e-mail: spayne@bionicsinstitute.org)

J.B.Fallon is with Bionics Institute, VIC 3002, Australia, Medical Bionics Department, University of Melbourne, VIC 3010, Australia and Department of Otolaryngology, University of Melbourne, VIC 3010, Australia (phone: (03) 9667 7500; e-mail: jfallon@bionicsinstitute.org)

I. Introduction

Significant interest has risen in the ability to harness the vagus nerve through electrical neuromodulation for the treatment of many diseases, such as epilepsy, depression, heart failure, obesity, inflammatory bowel disease, rheumatoid arthritis, type 2 diabetes and many more [1-3]. Our own efforts have investigated the use of vagus nerve stimulation in awake rats for the treatment of inflammatory bowel disease [4], rheumatoid arthritis [5] and type 2 diabetes [6]. Subsequently, our research supported the translation of the abdominal vagus nerve stimulation technology into a clinical trial for the treatment of Crohn's Disease (NCT05469607). When translating electrical neuromodulation technology, a critical step is the demonstration of long-term safety and efficacy in awake, freely moving preclinical rodent models.

Rat skull mount percutaneous connectors have most commonly been used in electrical neuromodulation studies relating to the brain [7] and cochlear [8, 9] for proximity to the target and rigidity of the skull when mounting a pedestal. When targeting the peripheral nervous system (PNS), implanted nerves are often located within the extremities or in the abdominal cavity. As such, routing a subcutaneous lead from the skull becomes surgically cumbersome, and following recovery a major potential point of failure arises around the neck due to forces occurring during animal movement. A solution used in our own PNS studies of awake rats is a percutaneous pedestal housing a commercial pin-to-socket connector mounted to the dorsal-lumbar aspect of the rat [4-6, 10]. Although electrically effective, commercially available pin-to-socket connectors require high connecting forces to mate and un-mate, which can stress the animal, impact on wounds around the plug, and requires significant training of the technician to connect the animal safely and efficiently.

This study describes the development and validation of a magnetically coupled percutaneous pedestal and external connector designed for chronic awake rat experiments utilizing the dorsal-lumbar i.e. back pedestal implantation site. Our design focuses on a) consisting of affordable components b) being reliable and safe for chronic implantation, c) easy to use by technicians and, d) easy to manufacture. We used biocompatible 3D printing, circuit board manufacturing, spring loaded pins for the electrical connection and magnets. The electrical connection between pedestal and cable was benchtop tested for continuity, durability and the disconnect forces of the assembly assessed. Using the magnetic percutaneous pedestal with an abdominal vagus nerve array,

similar to that used previously [11], the performance of the connection was tested *in vivo*. The reliability to stimulate and record from the vagus nerve through the connector was assessed by recording electrically evoked compound action potentials and continuity by impedance measurements of the electrodes.

II. Design

The chronic percutaneous connector was developed based on the feedback from research technicians that regularly connect and disconnect awake, freely moving animals for the purposes of chronic stimulation and recording, exampled in [4-6]. 3D printed components were designed in Fusion 360 (Fusion 360, AutoDesk, USA) and printed using a biocompatible resin printer (Form3B+, Formlabs, USA). Custom PCBs were designed and panelized in KiCad (KiCad 7.0).

A. Chronic Percutaneous Pedestal

The pedestal housing was printed with biocompatible material (Tough 1500, FormLabs, USA; Table I) with alignment notches to seat a custom 0.4 mm thick pedestal PCB (Fig. 1; Table I). The top of the pedestal PCB has a 4 mm diameter contact disc for soldering a samarium cobalt (SmCo) disc magnet (4 mm diameter x 2 mm height; Table I). This is circled by 10 contact discs on the top side which are routed to contact pads on the bottom for soldering lead wires to electrodes (Fig. 1, bottom view). The pedestal PCB is placed in the bottom recess of the housing and the remaining area is potted with biocompatible epoxy (EPO-TEK 353ND, Epoxy Technology, USA; Table I) to secure the components. Dacron mesh and silicon webbing (Table I) is cut (Cameo 4, Silhouette America, USA) and attached to the base of the pedestal. The silicone webbing provides rigidity to the Dacron mesh where tissue growth through pores of the mesh allows secure attachment of the pedestal following the healing process. The design of the pedestal is low profile to minimize damage from catching and reduce disruption to the animal's movement behavior. To prevent contamination or fouling of the contact discs within the pedestal, a magnetically secured protector (Fig. 1) was designed to seat within the socket of the pedestal when not actively in use.

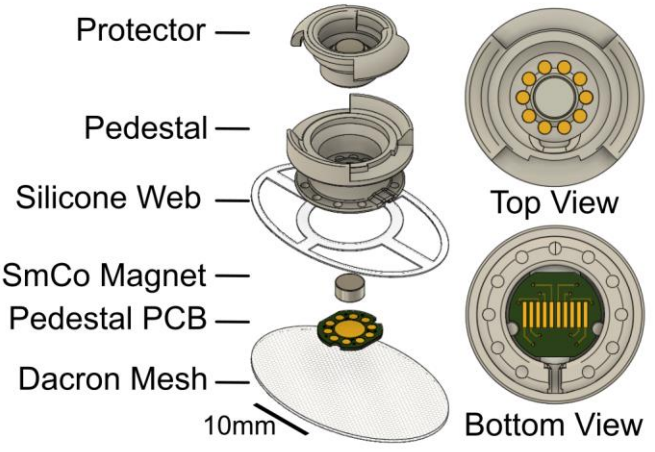

Fig. 1. Diagram of the chronic percutaneous pedestal assembly. Magnified top view showing contact discs of the pedestal PCB and bottom view of contact pads that implanted electrodes terminate to.

B. External Connector

The internal components of the external connector (Fig. 2) are 10 spring-loaded pins (Table I) aligned by an eternal connector PCB circling a large neodymium cylinder magnet (4 mm diameter x 6 mm height; Table I). Solder cup spring loaded pins were used to allow for solder attachment of a 10-core cable (1.8 mm diameter; Table I) that exits the top of the external connector. This is shrouded by a stainless-steel tension spring (0.3 mm diameter x 3mm O.D; Table I) to protect the wire from the animal when in use. All housings and internal components are secured using epoxy (Araldite, Selleys, Australia, Table I).

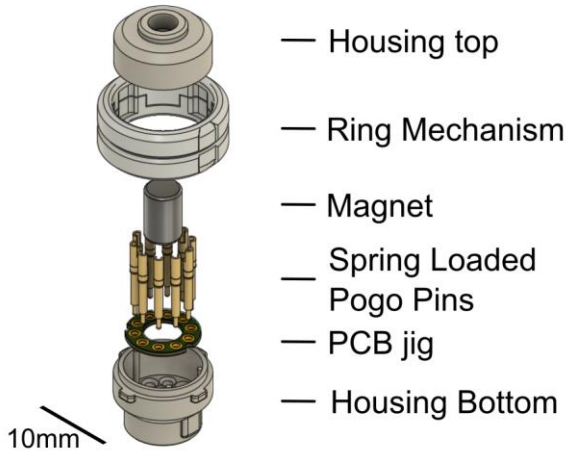

Fig. 2. Diagram of the external connector assembly. 10 spring-loaded pins are placed in an aligning PCB and circle a large neodymium magnet, encased in a 3D printed ring mechanisms to assist with disconnection.

C. Magnetic connection and disconnect mechanism

The connection mechanism between pedestal and external connector is achieved by magnetic coupling that draws the two design components together (Fig. 3, A). During disconnection, magnetic forces on the pedestal can be reduced by using a ring-mechanism that has a range of movement independent of the inner housing. Pulling force on the pedestal is displaced during disconnecting as the ring can be held stationary to prevent lifting of the pedestal as the external connector and pedestal magnets decouple (Fig. 3, B). This creates a clearance of 3.2 mm between the magnets of the pedestal and external connector, reducing the magnetic pulling force on the pedestal as ring and external connector are lifted away. The remaining magnetic forces when the ring-mechanism is engaged is low enough to allow for single handed disconnection and can be achieved without restraining the animal.

D. Assembly

A comprehensive breakdown of materials, product numbers and vendors can be found in Table I. Tools required to manufacture the pedestal and external connector include pairs of forceps (Micro-Adson forceps, 110118-12, Fine Science

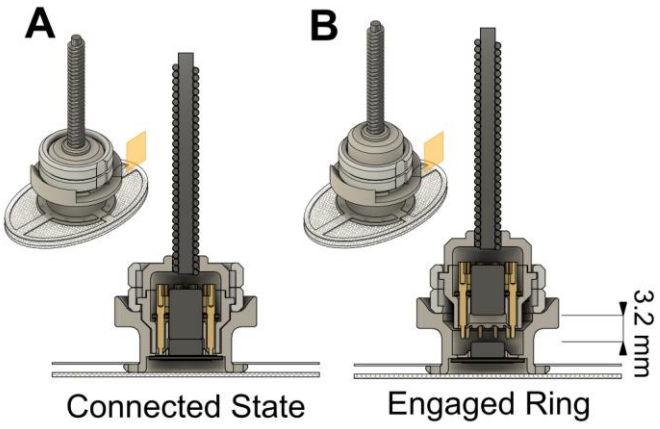

Fig. 3. Diagram and cross-sections of the two states of the external connector while connected to the pedestal. **A**. Normal connected state with magnetic components of pedestal and external connector in contact. **B**. With ring mechanism stabilized and cable pulled up, magnets are disconnected with a clearance of 3.2mm.

Tools, USA), microscope (Leican M80, Leica Microsystems, Germany) and soldering iron (ST 50, PACE, USA).

III. Methods

A. Benchtop testing

Two external connectors with cables and a pedestal mounted to a standard electrical component case (Fig. 4) were newly built for the purpose of benchtop testing. All 10 channels of the pedestal PCB were shorted to allow a single input voltage to be used as a dummy signal for testing purposes. For input signal recording during continuity and durability testing, a test rig (Fig. 4) was designed where the 10 wires of the spring-contact pins (1-10) from the external connector were attached to the digital input pins of a microcontroller (Arduino Uno pins 4-13, Arduino AG, BCMI, Italy) and each grounded with 10kΩ pull-down resistors. The microcontroller's 5V power pin was used to provide the dummy input signal to the pedestal. All microcontroller programming was written using Arduino Integrated Development Environment (Arduino AG 1.8.19, BCMI, Italy). Tests on each new cable were performed in the order of continuity, durability and disconnect force testing on the same pedestal.

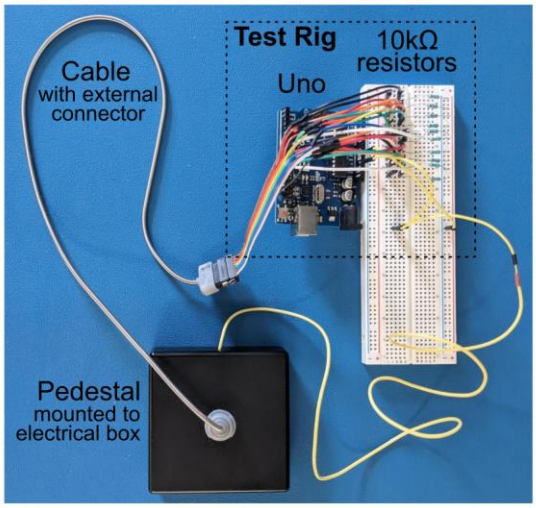

Fig. 4. Image of cable with external connector, pedestal mounted to electrical box and test rig including microcontroller and resistors layout used for benchtop testing.

1) Continuity Testing

To determine the reliability of the electrical connection of the design, a custom motorized system was built to mimic strain on the connector from animal movement. A 270° servo motor (DSS-M15S, DFRobot, China), controlled by a microcontroller (Adafruit Feather M0, Adafruit Industries, New York, USA) and a 3D-printed arm with slot to attach the connector cable, were used to generate randomized movement. The servo was powered at 5V, operating at a speed of 0.16 sec/60°. The microcontroller was programmed to perform continuous randomized sweeps at varying speeds and ranges. Speed was randomized by setting a random-length delay between motor control signal pulses of 10-30 ms, while range was randomized between 150-262.5° for positive direction sweeps, and 7.5-120° for negative direction sweeps.

During testing, the servo motor with attached arm was secured 150 mm above a large container which housed the pedestal. The external connector cable was plugged into the pedestal and attached to the servo arm at 95 mm from the axis of rotation. The cable was given minimal slack where movement of the arm would drag the pedestal inside the enclosure. The motorized system was then run continuously over the course of 1-hour, where the signal through each of the 10 connector pins was recorded by the test rig. The duration in milliseconds that each pin was connected or disconnected over the duration of the hour was measured and a percentage of successful connectivity attributed.

2) Durability testing

The durability of the design and electrical connection were tested through manually mating the pedestal and external connector 1000 times by a technician and continuity of all channels after each connect measured via the test rig. For each connect, once continuity was measured on any channel the test rig delayed 500 ms before taking a snapshot of continuity across all channels to account for pin bouncing. A Light Emitting Diode (LED) indicated when the connection was measured before the technician disconnected the device using the ring-mechanism and repeated the test. A successful connection was determined as all ten pins having continuity when measured, and a failed connection if any pin was disconnected. Each cable was attributed a percentage score for successful connections.

3) Disconnection force testing

To assess the force required to disconnect, the peak instantaneous force when un-mating the connection was measured with and without the ring mechanism of the external connector engaged. The external connector cable was plugged into the pedestal that was secured in position and a force gauge (Mark 10, M5-05, Mark 10 Corporation, New York, USA) attached to the cable of the external connector. The

force gauge was pulled vertically until disconnection occurred where peak tensile force was measured in Newtons and converted to force in grams. The ring mechanism was then locked in an engaged position (Fig. 3, B) using adhesive and peak tensile force to disconnect in this state measured. The disconnection force test was repeated 10 times for each state of the ring-mechanism and averaged.

B. *In vivo testing*

1) *Chronic abdominal vagus nerve electrode array*

A custom-made peripheral nerve array (Fig. 5, A) for rodent abdominal vagus nerve stimulation and recording was used for *in vivo* testing similar to that described previously [12]. The array consisted of 2-pairs of platinum electrodes (exposed surface area: 0.39 mm², distance between pairs: 4.7 mm) and a platinum ground ring mid-way up the lead-wire. The lead-wire consisted of platinum wires (50 µm diameter) from electrodes, which were soldered to the pedestal PCB and secured using biocompatible epoxy (353ND, Epoxy technology, USA). Pedestal and array were sonicated and sterilized by autoclave prior to implantation.

2) *Implantation surgery and euthanasia*

Animal procedures were approved by St Vincent's Hospital Animal Research Ethics Committee (Approval number: 002/24) and complied with the Australian Code for the Care and Use of Animals for Scientific Purposes (National Health and Medical Research Council of Australia) and the Prevention of Cruelty to Animals (1986) Act. Animals were housed in 390mm L x 250mm W x 250mm H containers, kept on a 12 h light/dark cycle and allowed access to standard chow and water *ad libitum*.

The surgical procedure takes less than 1.5 hours and is described in detail in Hyakumura *et al.* [12]. In brief, male Sprague-Dawley rats (n= 3, 10 weeks, Animal Resource Centre, Western Australia) were anaesthetized (induction: 3%, maintenance during surgery 2-2.5%, isoflurane, in oxygen flowing at 1 L/min) and administered analgesia (0.01 – 0.05mg/kg Buprenorphine, SQ; 5mg/kg Carprofen, SQ). A ventral abdominal midline incision was made, and the sub-diaphragmatic anterior abdominal branch of the vagus nerve exposed, and the peripheral nerve array implanted. The abdominal cavity was closed, and the percutaneous magnetic pedestal sutured to the dorsal lumbar aspect of the animal (Fig. 5, B). After a maximum of 3 weeks, rats were anaesthetized (3% isoflurane in 1 L/min oxygen) and euthanized (300 mg/kg Lethabarb, intracardiac injection).

3) *In vivo continuity testing and electrophysiological recordings*

In vivo continuity testing (via impedance measurements) and electrophysiological recordings were performed directly following implantation and twice a week up to 3-weeks from implantation in three animals while awake and freely moving within the confines of their housing enclosure. One animal was selected to extend the *in vivo* continuity measures to 3 weeks, the other animals were terminated at 2 weeks due to requirements of other experiments they were being utilized for.

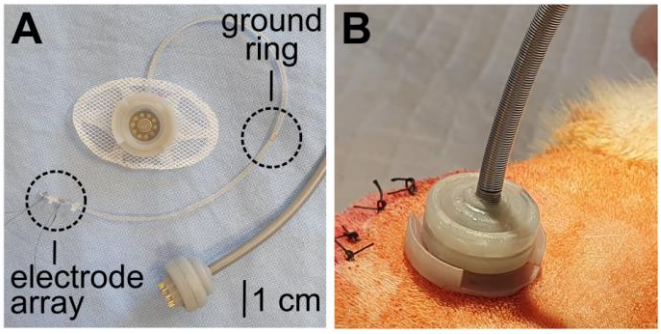

Fig. 5. **A.** Completed pedestal with rat abdominal vagus nerve electrode array, cable and ground ring. **B.** Implanted pedestal with external connector mated under anesthesia.

Common ground impedance measurements were taken at 30 second intervals over 1-hr to test continuity *in vivo* of the electrical connection during natural animal movement. Biphasic current (100 µA, 100 µs) pulses were passed between each electrode and all other electrodes using a custom stimulator [13]. The peak voltage at the end of the first phase (Vtotal) of the current pulse was measured, and the Vtotal value was used to calculate total impedance (Ztotal) using Ohm's law (Z = voltage/current). A percentage of successful connectivity was determined for each testing hour having 120 impedance measurements where inability to measure an impedance on any of the electrodes is considered unsuccessful.

Generation of evoked compound action potentials (ECAPs) were performed as described previously [14], where bipolar stimulation (10 Hz, 200 µs, 0-2 mA) was applied using a custom stimulator [13] across one pair of electrodes and evoked activity was amplified (ISO-80, World Precision Instruments, USA) and recorded (USB-6211, National Instruments, USA) via the second pair of electrodes. Recordings (sampled at 200 kHz) were digitally filtered (500–3000 Hz band pass), viewed and analyzed using IGOR Pro-9 software (IGOR v9.0, Wavemetrics, USA). The threshold of an evoked neural response is defined as the minimum current required to produce a waveform 0.1 V above baseline levels within a post-stimulus latency window of 4–10 ms. Signal to noise ratio (SNR) was calculated using the evoked response size at 2 mA stimulation versus noise floor and reported in decibels.

C. *Analysis*

Results are reported as average and standard error of mean. One Way Repeated Measures ANOVA was used for analysis (SigmaPlot v15, Inpixon).

IV. Results

A. *Material Cost analysis*

The cost of the materials required for manufacturing the two halves of the connector was calculated in USD (Table I). As the pedestal is considered a consumable, this was calculated separately to the external connector that can be continually used across multiple experiments. Shipping costs of materials were excluded from the calculation. The pedestal PCB and

TABLE I
MATERIAL COSTS

	Vendor	Bulk Amount	Bulk Cost	Amount Per Device	Cost Per Device
PERCUTANEOUS PEDESTAL					
Pedestal PCB	PCBWay	540	$116.45	1	$0.21
Magnet (4x2mm SmCo)	First4Magnets	200	$45.31	1	$0.23
FormLabs Tough 1500 Resin	FormLabs	1 L	$265.00	3.49 mL	$0.92
EPO-TEK 353ND	Epoxy Technology	236 mL	$145.00	1 mL	$0.61
Dacron Mesh	BioPlexus	6" x 8"	$104.00	1.7" x 1.1"	$3.96
Silicone Sheet (Reinforced)	BioPlexus	6" x 8" x 0.020"	$144.00	1.7" x 1.1"	$5.48
				Total Cost	**$11.41**
EXTERNAL CONNECTOR					
External Connector PCB	PCBWay	80	$116.45	1	$1.45
Spring loaded pin (0955-0-15-20-71-14-11-0)	MillMax	100	$73.21	10	$7.32
Magnet (N45 4x6mm)	AMF Magnetics	100	$41.49	1	$0.42
1.8mm Di. 10 core wire	-	50 m	$35.82	0.5 m	$0.56
Coil wire Shield (0.3mm x 3mm)	-	12 m	$14.39	0.5 m	$0.59
FormLabs Tough 1500 Resin	Formlabs	1 L	$265.00	3.16mL	$0.83
5 minute epoxy (Araldite)	Selleys	200 mL	$39.45	1 mL	$0.20
				Total Cost	**$11.37**

Material cost for percutaneous pedestal and external connector. Cost of materials in USD for bulk orders and individual cost per device.

external connector PCB were panelized onto a 100 mm x 80 mm PCB for bulk ordering. Ten panels were ordered where each panel consisted of 54 pedestal PCBs and 8 external connector PCBs. 3D printed material costs were calculated using the estimated volume of resin used by the printer software (PreForm, FormLabs, USA).

B. Bench Top Testing

1) Continuity testing

In cable one, 100% connectivity across all 10 channels was maintained for the duration of the 1-hr simulated animal movement. In cable two, nine of ten channels reported 100% connectivity. A single channel lost connectivity for 1.2 seconds a quarter of the way through the hour of testing. As a loss on any channel is considered disconnected, this has been reported as 99.96% continuity (Fig. 6, A).

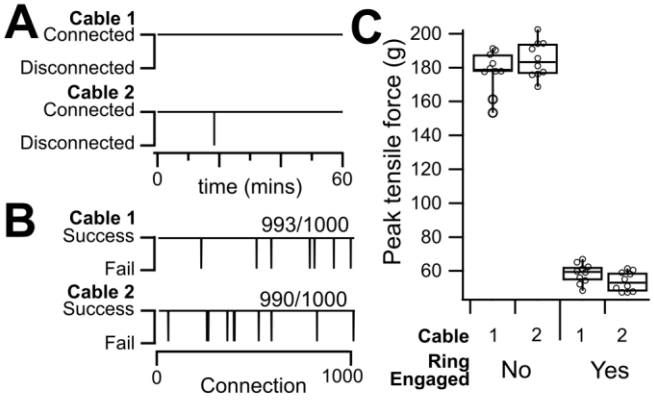

Fig. 6. *In vivo* ECAP results. **A.** ECAPs at implantation and 21 Days following implantation, blue window showing neural response. **B.** Neural response thresholds (µA) at implantation and subsequent awake recordings.

2) Durability testing

Cable one scored 99.3%, with successful connection of all ten channels in 993 out of 1000 tests performed. Cable two scored 99% with 990 out of 1000 successful connections. Failures did not increase towards the end of 1000 connections but occurred randomly throughout the test (Fig. 6, B).

3) Force testing

Testing in the normal connected state (ring not engaged), representative of the holding force of the connector, cable one averaged 178 ± 4 g to disconnect and cable two 184 ± 3 g (10 repeated test; Avg ± SEM; Fig. 6, C). With the ring mechanism locked in an engaged position, cable one averaged 59 ± 2 g and cable two averaged 54 ± 2 g (10 repeated tests; Avg ± SEM, Fig. 7, C).

C. In vivo continuity testing and electrophysiology

Continuity of the connection *in vivo* via 1-hr of continuous impedance testing was assessed in n=1 animal on days 5, 7, 12, 14, 18 and 21 post implantation. During testing, there was 100% connectivity on all four electrode channels during natural awake animal movement with the exception of day 5. A single electrode began the test disconnected, however 43 minutes into the hour the channel became connected and remained so for the remainder of the test. The resultant score for day 5 was reported as 28%.

ECAPs were successfully recorded in n=3 animals at surgery and for all awake recordings while implanted. At surgery, the average neural threshold was 1266 ± 133 µA (n=3; Avg ± SEM) and 733 ± 240 µA (n=3; Avg ± SEM) at last awake recording prior to termination, while the SNRs of the ECAP at those two timepoints were 31 ± 6 dB and 25 ± 6 dB respectively. A one-way repeated measure ANOVA showed there were no statistically significant difference ($F_{(2,4)}$ = 2.08; p = 0.240, n=3) in ECAP threshold across time (implantation, week 1 and week 2). In a representative example, ECAPs recorded following implantation elicited a

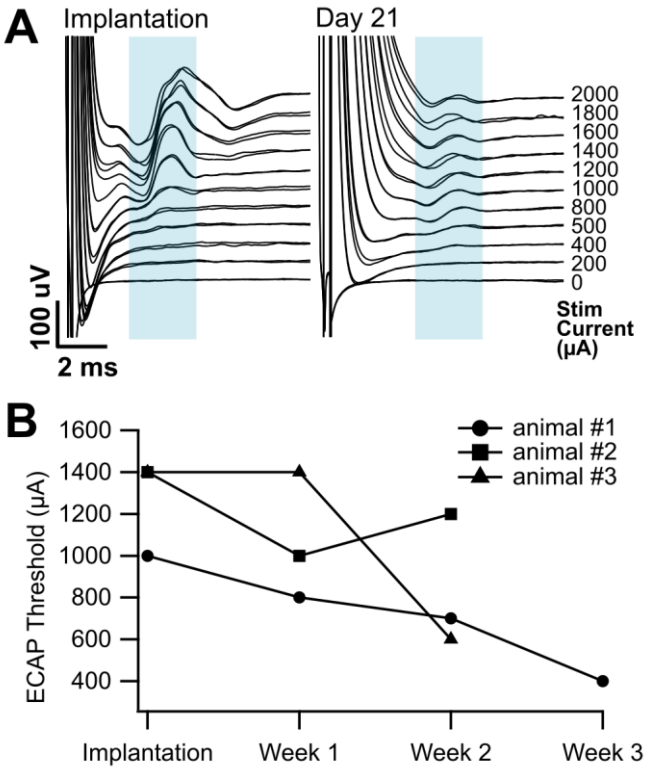

Fig. 7. *In vivo* ECAP results. **A.** ECAPs at implantation and 21 Days following implantation, blue window showing neural response. **B.** Neural response thresholds (µA) at implantation and subsequent awake recordings.

neural response with a latency of 4.4 ms, indicating a neural population with conduction velocity of ~1 m/s (Fig. 7, A). The ability to measure and record neural activity from the nerve remained robust throughout the implantation of all animals (Fig. 7, B) and quality of recording was not affected by awake animal movement.

Upon termination, we observed (n=3) no signs of irritation, damage or infection of the intradermal layers of the skin surrounding the pedestal.

V. Discussion

Here we developed and validated a percutaneous connector specifically designed for the dorsal-lumbar aspect of the spine of adult rats. The implanted pedestal and external connector are materially inexpensive with spring-loaded pins, magnets and biocompatible 3D printed housing that are easy to assemble. The magnetic coupling mechanism allows mating and disconnection with minimal force with high reliability of the electrical connection and minimal signal loss. When implanted in freely moving rats, the connector reliably delivered stimulation and received recording data from a peripheral nerve array throughout implantation.

Fully implantable stimulation and recording systems are available [15] and becoming increasingly advanced, however the design of a neural interface depends on the complexity of the neuroscientific research [16, 17]. Wireless stimulator and recording systems have advantages over percutaneous connectors, however they have a greater upfront cost requiring the miniaturized hardware for stimulation and recording per unit, usually deliver low sampling rates, have lower output current capabilities and battery life limitations. We have focused on optimizing the percutaneous connector as it offers greater flexibility to interface electrodes with larger external devices. This allows for more complex testing *in vivo* such as electrochemical characterization of electrodes [8], continuous stimulation for extended durations [18] and greater bandwidth for recording neural activity from multiple electrodes simultaneously [19].

Preclinical rodent neuromodulation studies often involve chronic or long-term implantation periods of 2-3 weeks [4] [5] [20, 21]. Chronic rodent experiments are technically challenging, partly due to animal size and early failure or migration of the implanted device. Developing a percutaneous connector requires consideration of the forces that will act on the pedestal to ensure that the design will last the duration of the experiment, is safe, can be mated without injuring the animal and excessive forces would not result in catastrophic injury. Depending on the anchoring mechanism and disconnect force required from the connector, unrecoverable injury or permanent damage to the connector can occur if excessive forces from the animal is applied while tethered. When measuring the disconnect force of our connector, it maintained a holding force of 181 grams (n=2) before detethering. As the average weight of Sprague-Dawley rats used experimentally is around 300-500 g [22], this holding force will be overcome in extreme circumstances that can cause significant injury to the animal or cause damage to the connector. Our magnetic anchor is therefore the appropriate balance between remaining safe and proving a stable connection during chronic stimulation and recording experiments.

The process of tethering an external connector to a percutaneous connector can be technically difficult for the user and potentially stressful to the animal. Minimizing the time and difficulty to connect serves to benefit welfare of the animal and save time of the researcher. Furthermore, animal handling can cause stress [23] detrimental to experiments that involve measuring animal behavioral responses [24]. An intuitive ring mechanism was developed around the external connector of our design that acts to stabilize the pedestal as the magnets are decoupled. The remaining magnetic force that is exerted on the pedestal once magnets are decoupled was measured at 56 grams (n=2). This force is negligible when disconnecting and can be achieved with one hand without disturbing the animal. Furthermore, the ring can be engaged prior to connecting and released once aligned with the pedestal, therefore exerting a maximum magnetic pulling force of 56 grams on the pedestal as the external connector approaches for mating. For comparison, an equivalent 10 channel pin-to-socket connector can require 2 kg of force to connect and a minimum of 200 g to disconnect [25].

As chronic implantations can last months, we tested beyond an average expectation of mating cycles to ensure durability of our device for long-term implantations. Each cable was mated and unmated with no notable damage or wear and tear to either pedestal or external connector. Failure to connect all 10

channels occurred sporadically rather than a degradation of the device towards the end of the test. Failed connections are likely due to pogo-pin bouncing where at the time of the snapshot of all channels, an electrical connection was not made. It was noted however when recreating this issue, once connected the channel would remain connected as seen *in vivo* on day 5 during an impedance continuity test.

To ensure effective therapeutic stimulation and reliable nerve recordings, the percutaneous connector must withstand natural animal movement without compromising signal integrity of the electrical connection. Our connector showed robust connectivity for all *in vivo* tests, with the exception of day 5's hour impedance continuity testing in one animal. Furthermore, ECAPs were successfully recorded in all implanted animals (n=3) and the latency of the evoked responses (4-10 ms) were consistent with a slow C-fibre neural population. Importantly, recordings remained consistent whether the animal was awake or under anesthesia, underscoring the connector's stability and minimal noise interference during awake animal movement.

The consumable pedestal component of our connector is cost effective ($11.41 USD) and simple to manufacture, indicated by a manufacturing time of less than 1 hour to assemble (excluding printing and curing times) and minimal equipment being required to assemble that does not require complex training to transfer manufacturing techniques to other technicians. The assembly is also biocompatible and sterilizable. The 3D printed component is made of tough biocompatible resin and uses an SmCo magnet that is rated up to 300 °C. This means that the percutaneous component can be autoclaved, sonicated and utilize thermally cured epoxy without effecting magnetic properties or warping the 3D printed housing. The external connector has a material cost of $11.37, requires several more hours to manufacture (approximately 2-3). The external connector however will last across multiple experiments, demonstrated to function for at least 1000 cycles without becoming damaged. Between animals, the materials of the external connector are safe to be cleaned using a sterile ethanol wipe. As the spring-loaded pins used in this design are rated for up to one million cycles [26], the external connector would be expected to last far beyond the 1000 cycles tested here. The cost of our percutaneous connector is accessible and simple to manufacture within a lab.

The low cost of our design limits it to 10 channels. This is permissible for peripheral nerve stimulation in rodents, however depending on the complexity of the neural stimulation or signal that is being recorded, access to a greater number of electrodes and therefore channels is required. Often connectors will have 16-256 connections however this can either increase the size of the connector or reduce the total number of cycles the connector can withstand as more delicate electrical interfaces are made [27]. While our design uses magnetics for the anchoring mechanism, this not only maintains the connection but is responsible for applying the compression force to each spring-loaded pin. As such, the interplay between magnetic forces and pin compression is crucial for scaling up our connector while preserving its functionality if the need for a greater number of channels was required.

VI. Conclusion

In conclusion, we have developed a novel low mating and un-mating force, high usability magnetic percutaneous connector for implantable peripheral nerve electrode arrays. Our materially cost-effective percutaneous connector demonstrates useability and robustness in withstanding natural animal movement and ensures uninterrupted delivery of stimulation and nerve recording signals. We anticipate the use of this connector will greatly improve the quality of pre-clinical research. In doing so, we have provided a research tool for peripheral nerve stimulation studies to allow investigation into the safety and efficacy of emerging neuromodulation therapies for the treatment of disease.

VII. Acknowledgments

We would like to acknowledge Mr. Ross Thomas for technical support for the plug design, Ms. Jenny Zhang for the manufacture of the array and Dr. Alex Thompson and Dr. David Hill for engineering expertise and support. We would also like to acknowledge members of the Animal Research Team for assistance in surgical procedures, animal care and husbandry.

VIII. Author contributions

All listed authors made substantial, direct and intellectual contributions to the study and manuscript, and were involved in reviewing the manuscript. Specifically, JVM was involved in conception and experimental design, acquisition and analysis of data, and was the primary writer of the manuscript; DTWW conducted bench top testing experiments and manuscript writing; JBF provided intellectual feedback on experimental design, engineering expertise and interpretation of data analysis; SCP was involved in conception, contributed to interpretation of results and was involved in significant drafting of the manuscript.

IX. Ethics statement

All animal procedures were approved by the Animal Research and Ethics Committee of St. Vincent's Hospital (reference number.: 002/24; approved 5 March 2024) and complied with the Australian Code for the Care and Use of Animals for Scientific Purposes (National Health and Medical Research Council of Australia).

X. Funding

Research reported in this publication was supported by the Bionics Institute Incubation Fund and from the National Health and Medical Research Council (APP2028605). The Bionics Institute acknowledge the support they receive from the Victorian Government through its Operational Infrastructural Support Program.

XI. Data Availability

The data that support the findings of this study are available from the corresponding author upon request.

The 3D models and PCB files used for making the percutaneous connector described in this paper have been made available online at https://github.com/Bionics-Institute-Public/PercPlug

XII. Disclosures

All authors declare no conflicts of interest, financial or otherwise.

XIII. References

[1] D. Guiraud *et al.*, "Vagus nerve stimulation: state of the art of stimulation and recording strategies to address autonomic function neuromodulation," *J Neural Eng*, vol. 13, no. 4, p. 041002, Aug 2016, doi: 10.1088/1741-2560/13/4/041002.

[2] M. Cracchiolo *et al.*, "Bioelectronic medicine for the autonomic nervous system: clinical applications and perspectives," *J Neural Eng*, vol. 18, no. 4, p. 1002, Mar 17 2021, doi: http://doi.org/10.1088/1741-2552/abe6b9.

[3] E. Ben-Menachem, "Vagus nerve stimulation, side effects, and long-term safety," *J Clin Neurophysiol*, vol. 18, no. 5, pp. 415-8, Sep 2001. [Online]. Available: http://www.ncbi.nlm.nih.gov/pubmed/11709646.

[4] S. C. Payne *et al.*, "Anti-inflammatory effects of abdominal vagus nerve stimulation on experimental intestinal inflammation," *Front Neurosci*, vol. 13, p. 418, 2019, doi: http://doi.org/10.3389/fnins.2019.00418.

[5] S. C. Payne *et al.*, "Abdominal vagus nerve stimulation alleviates collagen-induced arthritis in rats," *Front Neurosci*, vol. 16, p. 1012133, 2022, doi: 10.3389/fnins.2022.1012133.

[6] S. C. Payne *et al.*, "Blood glucose modulation and safety of efferent vagus nerve stimulation in a type 2 diabetic rat model," *Physiol Rep*, vol. 10, no. 8, 2022, doi: http://doi.org/10.14814/PHY2.15257

[7] T. Hyakumura *et al.*, "Improving Deep Brain Stimulation Electrode Performance in vivo Through Use of Conductive Hydrogel Coatings," *Front Neurosci*, vol. 15, p. 761525, 2021, doi: 10.3389/fnins.2021.761525.

[8] A. N. Dalrymple *et al.*, "Electrochemical and biological characterization of thin-film platinum-iridium alloy electrode coatings: a chronic in vivo study," *J Neural Eng*, vol. 17, no. 3, p. 036012, Jun 22 2020, doi: 10.1088/1741-2552/ab933d.

[9] M. R. Gold *et al.*, "Vagus nerve stimulation for the treatment of heart failure: The INOVATE-HF trial," *J. Am. Coll. Cardiol.*, vol. 68, no. 2, pp. 149-58, Jul 12 2016, doi: 10.1016/j.jacc.2016.03.525.

[10] S. C. Payne *et al.*, "Recording of electrically evoked neural activity and bladder pressure responses in awake rats chronically implanted with a pelvic nerve array," *Front Neurosci*, vol. 14, p. 619275, 2020, doi: http://doi.org/10.3389/fnins.2020.619275.

[11] S. C. Payne, G. Ward, R. J. MacIsaac, T. Hyakumura, J. B. Fallon, and J. Villalobos, "Differential effects of vagus nerve stimulation strategies on glycemia and pancreatic secretions," (in eng), *Physiol Rep*, vol. 8, no. 11, p. e14479, Jun 2020, doi: 10.14814/phy2.14479.

[12] T. Hyakumura, J. B. Fallon, and S. C. Payne, "Implantation surgery for abdominal vagus nerve stimulation and recording studies in awake rats," *J Vis Exp*, no. 203, Jan 19 2024, doi: 10.3791/65896.

[13] J. Fallon, P. Senn, and A. Thompson, "A highly configurable neurostimulator for chronic pre-clinical stimulation studies," in *Proceedings of the Neural Interfaces Conferences*, 2018.

[14] J. Fallon and S. Payne, "Electrophysiological recording of electrically-evoked compound action potentials," *protocols. io (20 October 2020)*, vol. 10, 2020.

[15] D. Perry *et al.*, "A fully implantable rodent neural stimulator," *Journal of neural engineering*, vol. 9, no. 1, p. 014001, 2012.

[16] F. Kohler *et al.*, "Closed-loop interaction with the cerebral cortex: a review of wireless implant technology," *Brain-Computer Interfaces*, vol. 4, no. 3, pp. 146-154, 2017.

[17] A. Deshmukh *et al.*, "Fully implantable neural recording and stimulation interfaces: Peripheral nerve interface applications," *Journal of Neuroscience Methods*, vol. 333, p. 108562, 2020.

[18] J. B. Fallon, D. R. F. Irvine, and R. K. Shepherd, "Cochlear implant use following neonatal deafness influences the cochleotopic organization of the primary auditory cortex in cats," *Journal of Comparative Neurology*, vol. 512, no. 1, pp. 101-114, 2009, doi: https://doi.org/10.1002/cne.21886.

[19] M. J. Francoeur *et al.*, "Chronic, Multi-Site Recordings Supported by Two Low-Cost, Stationary Probe Designs Optimized to Capture Either Single Unit or Local Field Potential Activity in Behaving Rats," (in eng), *Front Psychiatry*, vol. 12, p. 678103, 2021, doi: 10.3389/fpsyt.2021.678103.

[20] Y. A. Levine *et al.*, "Neurostimulation of the cholinergic anti-inflammatory pathway ameliorates disease in rat collagen-induced arthritis," *PLoS One*, vol. 9, no. 8, p. e104530, 2014, doi: 10.1371/journal.pone.0104530.

[21] J. Meregnani *et al.*, "Anti-inflammatory effect of vagus nerve stimulation in a rat model of inflammatory bowel disease," *Auton Neurosci*, vol. 160, no. 1-2, pp. 82-9, Feb 24 2011, doi: 10.1016/j.autneu.2010.10.007.

[22] C. L. Aleman *et al.*, "Reference database of the main physiological parameters in Sprague-Dawley rats from 6 to 32 months," *Lab Anim*, vol. 32, no. 4, pp.

457-66, Oct 1998, doi: 10.1258/002367798780599802.

[23] K. Gouveia and J. L. Hurst, "Optimising reliability of mouse performance in behavioural testing: the major role of non-aversive handling," *Scientific Reports*, vol. 7, no. 1, p. 44999, 2017/03/21 2017, doi: 10.1038/srep44999.

[24] R. M. J. Deacon, "Housing, husbandry and handling of rodents for behavioral experiments," *Nature Protocols*, vol. 1, no. 2, pp. 936-946, 2006/08/01 2006, doi: 10.1038/nprot.2006.120.

[25] HARWIN. *"M80 & M83 Series Rectangular Connector,"* C00541, Apr. 2024.

[26] MILL-MAX. *"0955-0-15-20-71-14-11-0 Data Sheet"*, 0955-0-15-20-71-14-11-0, May. 2024.

[27] C. F. Smith and K. S. Guillory, "High-Density, Low-Mating-Force, Magnetically-Coupled, Percutaneous Connector for Implanted Electrode Arrays," in *2007 3rd International IEEE/EMBS Conference on Neural Engineering, Neural Engineering, 2007. CNE '07. 3rd International IEEE/EMBS Conference on*, ed: IEEE, 2007, pp. 446-449.